Genes & Diseases (2023) 10, 1816–1819

Available online at www.sciencedirect.com

ScienceDirect

journal homepage: www.keaipublishing.com/en/journals/genes-diseases

RAPID COMMUNICATION

Biallelic mutations in *UGDH* cause congenital microcephaly

Hengel et al recently reported that bi-allelic loss-of-function mutations in UDP-Glucose 6-Dehydrogenase (*UGDH*) caused a severe epileptic encephalopathy syndrome-Jamuar syndrome (OMIM #618792).[1] The functional studies partially recapitulated the clinical phenotypes in the patient-derived cerebral organoid. A reduced number of proliferating neuronal progenitors in cerebral organoids was shown, which is a critical mechanism in congenital microcephaly (CM) whose patients were born with an occipitofrontal circumference (OCF) more than 2 standard deviations below average for age and sex. However, none of the reported patients in the article presented the phenotype as CM.

Here, we first identified *UGDH* compound heterozygous mutations (chr4:39523062-39523062 NM_003359.3:c.71C > T:p.A24V; chr4:39512342-39512342 NM_003359.3:c.404G > A:p.R135Q) in one family with CM by exome sequencing (ES) and Sanger validation. We then screened the Chigene database in China for additional CM patients with recessive *UGDH* mutations. Another patient with CM who also carried *UGDH* compound heterozygous mutations (chr4:39511460-39511460 NM_003359.3: c.731C > A: p.T244K; chr4: 39515798-39515798 NM_003359.3: c.169C > A: p.L57I) was identified (Fig. 1A, B; Fig. S1).

Patient 1 showed typical CM with progressively reduced OCF in pregnancy and OCF of 30.5 cm at 40 weeks of birth. He also showed core features of Jamuar syndrome by presenting developmental delay, severe refractory epilepsy-infantile spasms, and hypotonia accompanied by facial dysmorphisms such as flattened philtrum. Patient 2 also showed typical CM with OCF of 29.0 cm at 39 weeks of birth. He showed refractory epilepsy and severe developmental delay. Hypotonia was also detected. Magnetic resonance images (MRI) of the brain in both patients were normal.

These *UGDH* missense mutations were predicted to be likely pathogenic and highly conserved by multiple *in silico* tools (Table S1). The four variants are absent from normal population databases such as GnomAD, ExAC, and 1000genomes. The protein structure prediction (Fig. S2, 3A, B) showed that the angles and distances between *UGDH* mutants and the contact atoms were different from wild-type UGDH. For p.T244K mutant, one of the interaction molecules has changed from A246 to K465 (Fig. S3B). These may indicate that UGDH mutants could lead to altered local structure, thus affecting UGDH enzyme functions.

UGDH enzymatic activity was further measured by the activity of NADH oxidase assay accompanied with trypsin susceptibility assay and thermal stability measurement. As shown in Fig. 1C, we found that the efficiency of conversion of NAD^+ to NADH was reduced when comparing UGDH A24V and R135Q (Patient 1) group with UGDH WT group (62% ($P < 0.0001$) and 39% ($P < 0.0005$)). For patient 2 with UGDH L57I and T244K (Fig. 1D), the reduction in efficiency of conversion of NAD^+ to NADH as compared to UGDH WT were 46% ($P < 0.0005$) and 55% ($P < 0.0001$) respectively. We further found that the *UGDH* missense mutations may reduce the enzymatic oxidoreductive activity by affecting its sensitivity to proteolysis and/or thermal stability (Fig. S2, 3C, D). These results suggested a loss-of-function mechanism underlying *UGDH* missense mutations.

Therefore, we constructed *UGDH* knockout HEK293T cell models to elucidate the pathogenesis of *UGDH*. In order to explore the key proteins or pathways regulated by *UGDH* mutations, TMT labeled quantitative proteomic analysis on *UGDH* knockout and wild-type HEK293T cells was applied. A total of 7,772 proteins were identified, out of which the number of quantifiable proteins was 7,769. Taking the fold change (FC) > 1.2 times (up-regulation greater than 1.2 times or down-regulation less than 0.83 times) and *P*-value < 0.05 as the standard, the number of up-regulated and down-regulated proteins between groups was 575 and 535, respectively (Fig. S4A). Gene ontology analysis of biological processes showed that the differentially expressed protein may be enriched in functional categories including cell proliferation, developmental process, etc (Fig. S4B). The Kyoto Encyclopedia of Genes and Genomes pathway analysis showed that the

Peer review under responsibility of Chongqing Medical University.

https://doi.org/10.1016/j.gendis.2022.12.007

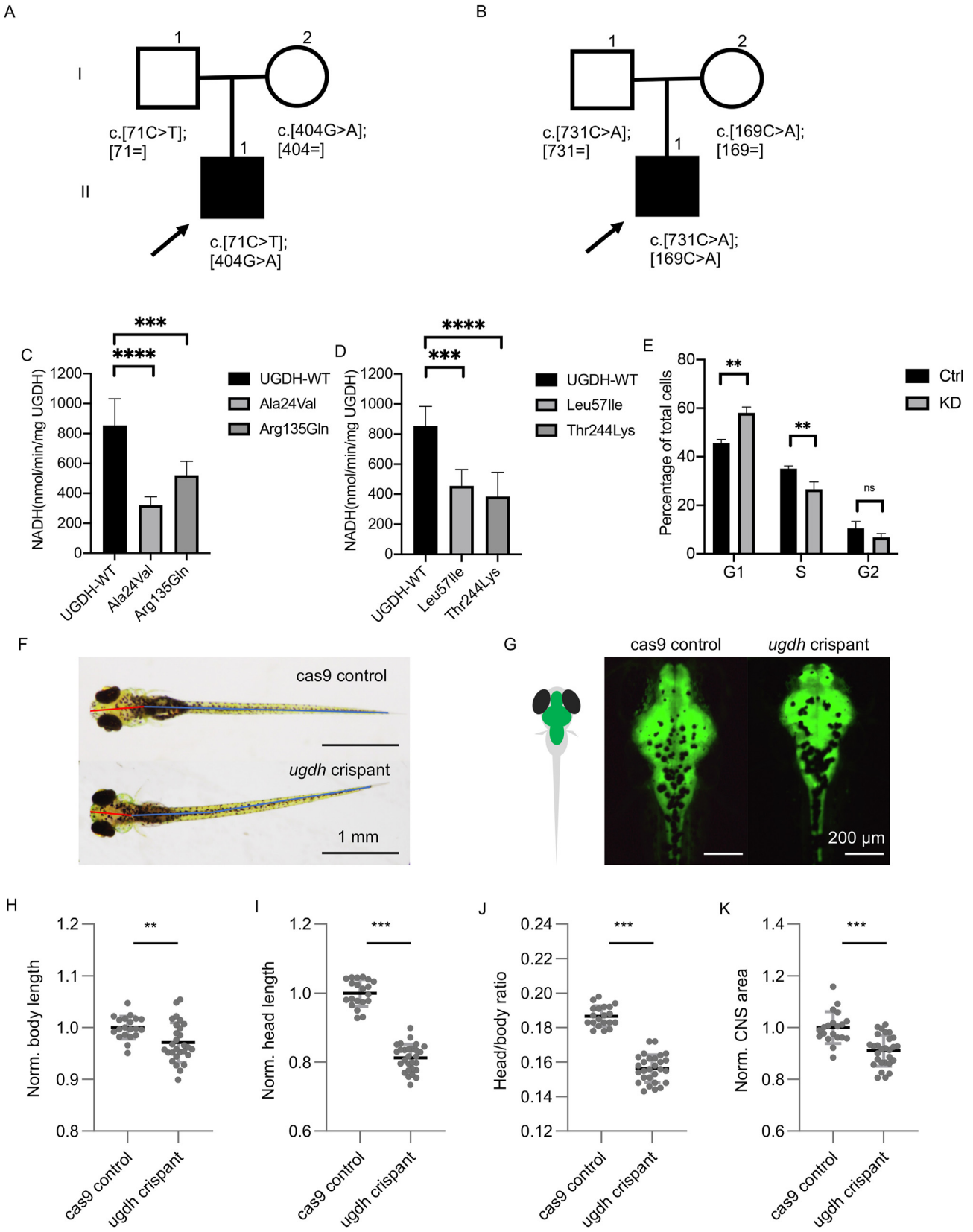

Figure 1 Compound heterozygous mutations in the *UGDH* gene caused decreased enzymatic activity, interruption of the cell cycle, small brain and neuronal loss in zebrafish F0 crispant. **(A)** The pedigree of family 1 segregates CM. The arrow points to the proband. Compound heterozygous mutations c.71C > T and c.404G > A in *UGDH* are presented below individuals. **(B)** The pedigree of the family 2 segregates CM. The arrow points to the proband.Compound heterozygous mutations c.169C > A and c.731C > A in

differentially expressed protein was enriched in the cell cycle pathway etc (Fig. S4C).

In accordance with the proteomic analysis, cell cycle analysis showed that the loss of function of *UGDH* resulted in the interruption of the cell cycle transition from the G1 to the S phase. We used *UGDH* knockdown HEK293 cell models and found that there were about 9% more cells in the G1 phase and about 9% fewer cells in the S phase in the gene knockdown group than in the control group ($P < 0.05$). However, the percentage of cells in G2/M between the two groups has no statistically significant difference (Fig. 1E).

To further evaluate the function of *UGDH* in brain development, we obtained RNA sequencing data from BrainSpan. The Spatio-temporal expression pattern of *UGDH* suggested that there is a time-dependent down-regulation of UGDH expression in the fetal brain and in the postnatal brain. The high expression level was observed in fetal periods in most brain regions (Fig. S5A, B). The result implicated a major role of UGDH in brain development during embryonic development periods. In the zebrafish model, significant differences of head length, body length, head-to-body length ratio, and central nervous system fluorescence area were observed between cas9 injected control and *ugdh* first generation (F0) crispant ($P < 0.01$, 0.001, 0.001, 0.001, respectively) (Fig. 1F–K). The F0 crispant simulated CM by showing small brain and neuronal loss.

UGDH (MIM603370) is a vital enzyme that catalyzes UDP-glucose to UDP-glucuronate accompanied by NAD^+ to NADH. Its downstream product-the extracellular matrix glycosaminoglycan component hyaluronan is essential for multiple cell functions.[2] As a crucial gene functioning in the neurological system, *UGDH* mutations were first proved to be causative to developmental and epileptic encephalopathy 84-Jamuar syndrome by Hengel et al in 2020.[1] The zebrafish model developed by the author did not phenocopy the clinical features of the phenotypes of patients satisfactorily by only simulating the motor developmental delay. Additionally, Hengel et al found a reduced volume of patient-derived cerebral organoids due to decreased number of neuroprogenitors (NPCs).

Not only does the finding indicate the importance of *UGDH* in neurodevelopment, but it also coincided with the core pathogenesis underlying CM. The CM phenotype was not shown in the patients reported by Hengel et al. Fortunately, we identified two patients with CM accompanied by developmental delay and refractory seizures who harbored *UGDH* compound heterozygous mutations, therefore, to make the clinical presentations of patients more congruent with functional studies.

The protein structure prediction indicated that the protein stability and enzymatic function were affected by *UGDH* mutations. The angles, distances, and interaction molecules were changed by *UGDH* mutations which could result in impaired enzyme functions and downstream products. In accordance with the structure prediction, the lower level of UGDH enzyme activities caused by *UGDH* missense mutations also indicated the loss-of-function mechanisms of these missense mutations.

Furthermore, the quantitative proteomic analysis and *UGDH* knockdown cell models showed that the disturbed cell cycle may be the underlying mechanism in *UGDH*-related microcephaly. The bioinformatics analysis showed the importance of UGDH in brain development in embryonic development periods and *ugdh* F0 CRISPR (crispant) presented reduced brain volume and central nervous system (CNS) area. In accordance with patient-derived cerebral organoids in a previous study, which showed a markedly reduced number of NPCs and small volume, all supported the role of *UGDH* in CM pathogenesis.

As a crucial gene-regulating proteoglycan (PG) and glycosaminoglycan (GAG) synthesis, UGDH is critical throughout cell development. It has been reported that in diverse organisms such as flies, worms, and plants, UGDH loss could result in limited developmental growth. For example, by interrupting downstream factors including Wnt, fibroblast growth factor, and transforming growth factor-β, phenotypes such as wing dysplasia in *Drosophila* were detected.[3] UGDH could implicate human diseases by affecting PG or GAG levels of the extracellular matrix and thus affecting tissue morphogenesis.[2] Inborn errors of proteoglycan metabolism could cause multiorgan impairments. So far, only three studies have reported *UGDH*-related congenital developmental diseases, including cardiac valve malformation and developmental, epileptic encephalopathy, and developmental delay.[1,4,5] Our study is the first report to unravel the role of *UGDH* in CM.

Therefore, given the above data, together with the reduced number of NPCs in cerebral organoids presented by Hengel et al, we proposed that *UGDH* mutation is likely to cause CM.

UGDH are presented below individuals. **(C, D)** Purified UGDH wild-type (WT) and mutant enzymatic activity. (C) A24V and R135Q in patient 1 and (D) L57I and T244K in patient 2 were measured as the turnover of NAD^+ to NADH. The assay was performed by at least three replicate experiments. **(E)** Percentage of cells in different phases of the cell cycle (G0/G1, S, G2/M). KD, *UGDH* knockdown HEK293 cell. Ctrl, controls. $^{**}P < 0.01$, $^{***}P < 0.001$, $^{****}P < 0.0001$; student's *t*-test. ns indicates no significance with a *P*-value >0.05. **(F)** Representative bright-field imaging of larval zebrafish at 5 days after fertilization (dorsal view). Top, cas9 injected control; bottom, *ugdh* F0 CRISPR (crispant). The Red plus blue line indicates the body length and the red line indicates the head length. **(G)** Representative imaging of HuC: eGFP-expressed larval zebrafish shows CNS fluorescence pattern at 5 after fertilization (dorsal view). Left, cas9 injected control; right, *ugdh* crispant. **(H–J)** Measurements of body length, head length, and the head-to-body length ratio in cas9 injected control ($n = 20$ fish) versus *ugdh* crispant ($n = 28$ fish). Body length and head length data were normalized to the mean value of cas9 control group. **(K)** Normalized CNS fluorescence area in cas9 injected control ($n = 20$ fish) versus *ugdh* crispant ($n = 28$ fish). Scale bars are indicated in the figure. Error bars indicate standard deviation (SD). Statistical significance is indicated as $^{*}P < 0.05$, $^{**}P < 0.01$, $^{***}P < 0.001$.

Author contributions

XM and HW designed the research. LS wrote the manuscript. DQM provided information on one patient. RX performed the bioinformatic analysis. GYX, SXL, and XL collected and evaluated the clinical and genetic evidence. BX and YYX revised the manuscript. All authors read and approved the final manuscript.

Conflict of interests

All authors declare that there is no conflict of interests.

Funding

This work was supported by the Natural Science Foundation of Hunan Province, China (No. 2021JJ40280), the National Key Research and Development Program of China (No. 2021YFC1005300), the Major Scientific and Technological Projects for Collaborative Prevention and Control of Birth Defects in Hunan Province, China (No. 2019SK1010, 2019SK1014), the National Key R&D Program of China (No. 2019YFC1005100), the Hunan Provincial Science and Technology Department (China) (No. 2018SK2064), the Joint Construction Project of Henan Medical Science and Technology Project (China) (No. LHGJ20200618, 2018020633), and the Henan Engineering Research Center of Childhood Neurodevelopment Open Project (China) (No. SG201907).

Acknowledgements

We thank all the participated patients and their families for their cooperation, as well as our cooperative organization Chigene (Beijing) Translational Medical Research Center Co. Ltd.

Appendix A. Supplementary data

Supplementary data to this article can be found online at https://doi.org/10.1016/j.gendis.2022.12.007.

References

1. Hengel H, Bosso-Lefèvre C, Grady G, et al. Loss-of-function mutations in UDP-Glucose 6-Dehydrogenase cause recessive developmental epileptic encephalopathy. *Nat Commun*. 2020;11(1):595.
2. Zimmer BM, Barycki JJ, Simpson MA. Integration of sugar metabolism and proteoglycan synthesis by UDP-glucose dehydrogenase. *J Histochem Cytochem*. 2021;69(1):13—23.
3. Häcker U, Lin X, Perrimon N. The *Drosophila* sugarless gene modulates Wingless signaling and encodes an enzyme involved in polysaccharide biosynthesis. *Development*. 1997;124(18):3565—3573.
4. Hyde AS, Farmer EL, Easley KE, et al. UDP-glucose dehydrogenase polymorphisms from patients with congenital heart valve defects disrupt enzyme stability and quaternary assembly. *J Biol Chem*. 2012;287(39):32708—32716.
5. Alhamoudi KM, Bhat J, Nashabat M, et al. A missense mutation in the *UGDH* gene is associated with developmental delay and axial hypotonia. *Front Pediatr*. 2020;8:71.

Li Shu [a,b,c,1], Guangyao Xie [a,1], Daoqi Mei [d,1], Rui Xu [e], Shixian Liu [f], Bo Xiao [g], Xing Li [h], Yuanyuan Xie [g,***], Xiao Mao [a,i,j,**], Hua Wang [k,*]

[a] *National Health Commission Key Laboratory for Birth Defect Research and Prevention, Hunan Provincial Maternal and Child Health Care Hospital, Changsha, Hunan 410005, China*
[b] *Departments of Biochemistry, Molecular Biology and Medical Genetics, Cumming School of Medicine, University of Calgary, Calgary T2N 4N1, Canada*
[c] *Alberta Children's Hospital Research Institute, University of Calgary, Calgary T2N 4N1, Canada*
[d] *Department of Neurology, Children's Hospital Affiliated to Zhengzhou University, Zhengzhou, Henan 450018, China*
[e] *Department of Cell Biology and Genetics, School of Basic Medical Science, Xinjiang Medical University, Urumqi, Xinjiang 830054, China*
[f] *Department of Pediatric Neurological and Rehabilitation, Ganzhou Women and Children's Health Care Hospital, Ganzhou, Jiangxi 341000, China*
[g] *Department of Neurology, Xiangya Hospital, Changsha, Hunan 410005, China*
[h] *Department of Pediatrics, The First Affiliated Hospital of Guangxi Medical University, Nanning, Guangxi 530021, China*
[i] *Department of Medical Genetics, Hunan Provincial Maternal and Child Health Care Hospital, Changsha, Hunan 410005, China*
[j] *Clinical Research Center for Placental Medicine in Hunan Province, Hunan Provincial Maternal and Child Health Care Hospital, Changsha, Hunan 410005, China*
[k] *Department of Medical Genetics, Hunan Children's Hospital, Changsha, Hunan 410007, China*

*Corresponding author.

**Corresponding author. National Health Commission Key Laboratory for Birth Defect Research and Prevention, Hunan Provincial Maternal and Child Health Care Hospital, Changsha, Hunan 410005, China.

***Corresponding author.
E-mail addresses: 55651829@qq.com (Y. Xie), gbtechies@outlook.com (X. Mao), wanghua_213@hotmail.com (H. Wang)

18 April 2022
Available online 11 January 2023

[1] These authors have contributed equally to this work and are co-first authors.